

Xueyong Xu,^{a,b} Xiaoyan Wang,^{a,b}
Jingjin Ding^{a*} and Da-Cheng
Wang^{a*}

^aNational Laboratory of Biomacromolecules,
Institute of Biophysics, Chinese Academy of
Sciences, Beijing 100101, People's Republic of
China, and ^bGraduate University of Chinese
Academy of Sciences, Beijing 100039,
People's Republic of China

Correspondence e-mail: jding@moon.ibp.ac.cn,
dcwang@ibp.ac.cn

Received 6 March 2012

Accepted 17 April 2012

Crystallization and preliminary crystallographic studies of CCM3 in complex with the C-terminal domain of MST4

MST4 is a member of the GCKIII kinases. The interaction between cerebral cavernous malformation 3 (CCM3) and GCKIII kinases plays a critical role in cardiovascular development and in cerebral cavernous malformations. The complex of CCM3 and the C-terminal domain of MST4 has been constructed, purified and crystallized, and a diffraction data set has been collected to 2.4 Å resolution. The crystal of the CCM3–MST4 C-terminal domain complex belonged to space group $P4_12_12$ or $P4_32_12$, with unit-cell parameters $a = 69.10$, $b = 69.10$, $c = 117.57$ Å.

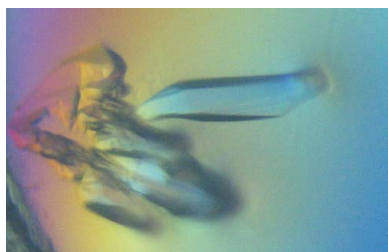
1. Introduction

Cerebral cavernous malformations (CCMs) affect 0.1–0.5% of the general population. CCMs are characterized by abnormally enlarged thin-walled vessels lined by a monolayer of endothelial cells with no underlying smooth muscle. Bleeding frequently occurs in these lesions, and they can lead to stroke, seizure, various types of neurological disorder and even death. Familial CCMs are linked to mutations in three CCM genes: *ccm1–3* (Revencu & Vikkula, 2006). The proteins encoded by these three genes can interact with one another (Voss *et al.*, 2007; Zawistowski *et al.*, 2005), implying that they may share a common biochemical function.

ccm3 is the least understood of the three *ccm* genes. It was initially characterized as an apoptosis-related gene. Loss-of-function mutations cause an enlarged-heart phenotype in zebrafish (Zheng *et al.*, 2010) and defects in early angiogenesis and early embryonic lethality in mouse (He *et al.*, 2010). CCM3 has been identified to participate in vascular development by stabilizing vascular endothelial growth factor receptor 2 (VEGFR2) signalling (He *et al.*, 2010) and by mediating germinal centre kinase class III (GCKIII) kinase signalling (Zheng *et al.*, 2010). It also can regulate neuronal survival and the activation of astrocytes (Louvi *et al.*, 2011).

The GCKIII subfamily of proteins includes MST4, STK24 and STK25. GCKIII kinases play critical roles in many cellular processes, including cell growth, orientation, migration and polarization. By interacting with the Golgi matrix protein GM130, all three GCKIII kinases can be located at the Golgi apparatus; they can be activated through homodimerization and thus regulate Golgi assembly and adequate orientation of the centrosome and Golgi (Fidalgo *et al.*, 2010).

CCM3 contains two domains: an N-terminal homodimerization domain and a C-terminal focal adhesion targeting (FAT) homology domain. Each GCKIII kinase consists of an N-terminal catalytic domain and a C-terminal regulatory region (GCKIIIct). Recent studies have shown that the N-terminal domain of CCM3 directly interacts with the C-terminal regulatory regions of GCKIII kinases (Ceccarelli *et al.*, 2011). The interactions between CCM3 and GCKIII kinases play important roles in Golgi assembly, cell orientation and endothelial cell–cell junctions. They not only stabilize the activated



GCKIII kinases, but also negatively regulate Rho by directly activating moesin (Fidalgo *et al.*, 2010; Zheng *et al.*, 2010). Additionally, striatins and CCM3 can act as adapter molecules to bridge the GCKIIIs and a higher order complex termed STRIPAK (striatin-interacting phosphatase and kinase; Goudreault *et al.*, 2009). This complex can regulate the localization of GCKIII kinases in the cell to control Golgi positioning.

To date, although there is an increasing understanding of the biochemical properties and physiological roles of the interactions between CCM3 and GCKIII kinases, the structural basis of their interactions has remained puzzling. We have constructed and purified the complex of CCM3 and the C-terminal domain of MST4 and here we report the crystallization, diffraction data collection and preliminary crystallographic studies of this complex.

2. Materials and methods

2.1. Cloning, expression and purification

The DNA fragment encoding residues 8–212 of human CCM3 was amplified by polymerase chain reaction (PCR) and the fragment was cloned into the pET-22b(+) expression vector (Novagen) and placed between *NdeI* and *XhoI* restriction sites. A six-histidine tag (LEH-HHHHH) was engineered into the C-terminus of the protein. The DNA encoding the C-terminal regulatory tail of human MST4 comprising residues 346–416 was amplified by PCR and the DNA fragment was cloned into pET-32M-3C expression vector and placed between *BamHI* and *NotI* restriction sites. A thioredoxin and six-histidine tag and a PreScission protease site were engineered into the N-terminus of the protein. The pET-22b(+)-CCM3 plasmid was transformed into *Escherichia coli* BL21 (DE3) strain competent cells, which were then grown on LB plates supplemented with 100 mg ml⁻¹ ampicillin at 310 K overnight. A single colony was used to inoculate 50 ml LB medium, which was cultured overnight. 24 ml of the bacterial culture was then transferred into 800 ml fresh LB medium. The cells were induced with 0.25 mM isopropyl β -D-1-thiogalactopyranoside (IPTG) when the culture reached an OD₆₀₀ of 0.6–1.0. After induction, cell growth was continued for 18 h at 291 K. The C-terminal regulatory tail of MST4 was expressed in the same way as CCM3. The cells were harvested by centrifugation, and the bacterial pellets that expressed CCM3 and the bacterial pellets that expressed the MST4 C-terminal domain were resuspended in lysis buffer (20 mM HEPES pH 7.5, 400 mM sodium chloride, 5 mM imidazole, 5 mM β -mercaptoethanol), mixed together and disrupted by ultrasonication. The lysate was centrifuged at 24 000g and 277 K for 40 min. The supernatant was loaded onto an Ni-NTA column (Novagen) pre-equilibrated with lysis buffer. The column was washed with wash buffer (20 mM HEPES pH 7.5, 400 mM sodium chloride, 20 mM imidazole, 5 mM β -mercaptoethanol) and the complex was eluted with elution buffer (20 mM HEPES pH 7.5, 400 mM sodium chloride, 250 mM imidazole, 5 mM β -mercaptoethanol). The eluate was concentrated to 1 ml by ultrafiltration (Millipore) at 277 K, supplemented with 50 ml lysis buffer and then concentrated to 1 ml again. The thioredoxin and six-histidine tag was cleaved from the MST4 C-terminal domain with PreScission protease for 10 h. The sample was then diluted with 15 ml lysis buffer and purified on an Ni-NTA column (Novagen) using the same approach as described above; the eluate was again concentrated to 1 ml by ultrafiltration (Millipore) at 277 K. The sample was then loaded onto a Superdex 75 HiLoad 16/60 column (GE Healthcare) previously equilibrated with 25 mM HEPES pH 7.5, 150 mM sodium chloride, 2 mM DTT. The

peak corresponding to the complex was collected, concentrated, flash-cooled to 77 K in liquid nitrogen and stored at 193 K.

2.2. Crystallization

The complex was concentrated to approximately 60 mg ml⁻¹. Protein concentrations were determined from the absorbance at 280 nm. Initial crystallization screening was set up using the hanging-drop vapour-diffusion method with the Index screen from Hampton Research by mixing 1 μ l protein solution and 1 μ l reservoir solution and suspending the drop over 0.5 ml reservoir solution at 293 K. The crystallization conditions were optimized by varying the type and the concentration of the precipitant (PEG), salts, buffers and organic compounds and the pH.

2.3. Data collection and processing

Diffraction data were collected from crystals of the complex with Cu K α wavelength radiation ($\lambda = 1.5418$ Å) using a Rigaku R-AXIS IV⁺⁺ image-plate system mounted on a rotating-anode X-ray source operating at 40 kV and 20 mA with 0.1 mm confocal incident-beam diameter at the National Laboratory of Biomacromolecules, Institute of Biophysics, Chinese Academy of Sciences. *MOSFLM* (v.7.0.4; Leslie, 2006) and *SCALA* (v.6.0) from the *CCP4* program suite (v.6.0.2; Winn *et al.*, 2011) were used for processing, reduction and scaling of the diffraction data.

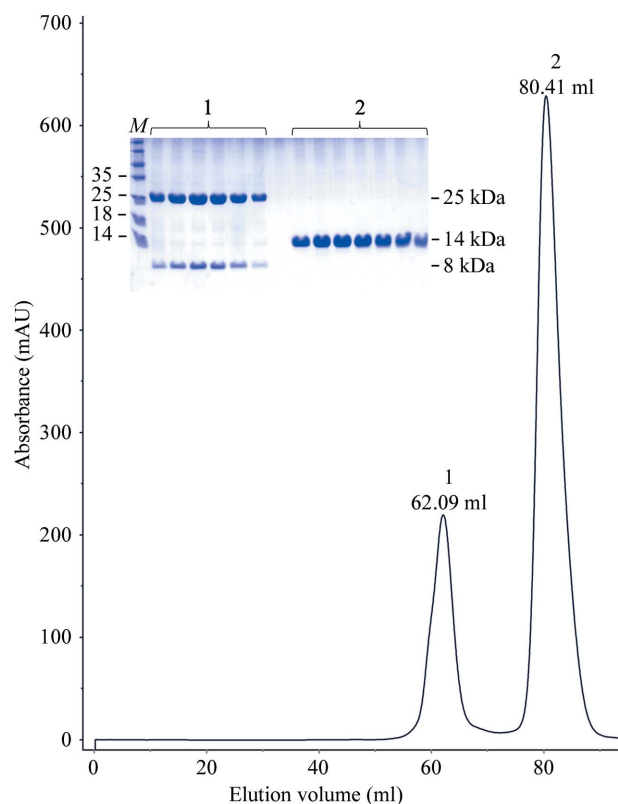


Figure 1 Elution profiles of purification of the complex of CCM3 and the MST4 C-terminal domain using a Superdex 75 HiLoad 16/60 column (GE Healthcare). Peak 1 corresponds to the complex of CCM3 (25 kDa) and the MST4 C-terminal domain (8 kDa); peak 2 corresponds to the six-histidine and thioredoxin tag of the MST4 C-terminal domain (14 kDa). Insert, SDS-PAGE gel (15%) of the corresponding purified protein from each peak. Lane M contains molecular-weight markers (labelled in kDa).



Figure 2
Crystal of the complex of CCM3 and the MST4 C-terminal domain.

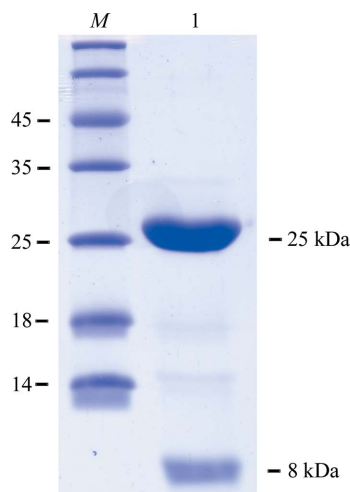


Figure 3
SDS-PAGE of the dissolved crystals. Lane *M*, molecular-weight markers (labelled in kDa); lane 1, the dissolved crystals, which were comprised of CCM3 (25 kDa) and MST4 C-terminal domain (8 kDa).

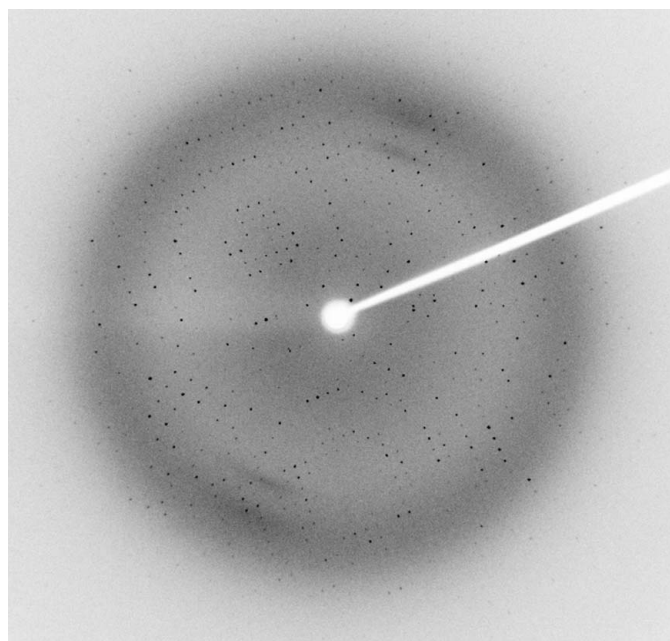


Figure 4
Diffraction pattern of a crystal of the complex of CCM3 and the MST4 C-terminal domain.

Table 1

Data-collection statistics for the crystal of the complex of CCM3 and the MST4 C-terminal domain.

Values in parentheses are for the highest resolution shell.

Space group	$P4_12_12$ or $P4_32_12$
Unit-cell parameters	
<i>a</i> (Å)	69.10
<i>b</i> (Å)	69.10
<i>c</i> (Å)	117.57
Wavelength (Å)	1.5418
Resolution (Å)	45.12–2.40 (2.53–2.40)
No. of unique reflections	11591
$R_{\text{merge}}^{\dagger}$ (%)	7.6 (35.3)
Multiplicity	6.9 (6.7)
Molecules per asymmetric unit	1
V_M (Å ³ Da ⁻¹)	2.13
Average $I/\sigma(I)$	27.3 (7.4)
Completeness (%)	100 (100)
Wilson <i>B</i> factor (Å ²)	37.575

$\dagger R_{\text{merge}} = \frac{\sum_{hkl} \sum_i |I_i(hkl) - \langle I(hkl) \rangle|}{\sum_{hkl} \sum_i I_i(hkl)}$, where $\langle I(hkl) \rangle$ is the mean of the observations $I_i(hkl)$ of reflection hkl .

3. Results

The complex was finally purified using a Superdex 75 HiLoad 16/60 column (Fig. 1). The elution profile showed two peaks: peak 1 corresponds to the complex of CCM3 and the MST4 C-terminal domain (33 kDa), while peak 2 corresponds to the thioredoxin and six-histidine tag of the MST4 C-terminal domain (14 kDa). SDS-PAGE was used to confirm the presence of the complex and showed two bands corresponding to the molecular weights of CCM3 (25 kDa) and the MST4 C-terminal domain (8 kDa).

Crystals were initially obtained using Index conditions No. 70 [0.2 *M* sodium chloride, 0.1 *M* bis-Tris pH 5.5, 25% (w/v) polyethylene glycol 3350] and No. 78 [0.2 *M* ammonium acetate, 0.1 *M* bis-Tris pH 5.5, 25% (w/v) polyethylene glycol 3350]. Crystals were observed after 3 d (Fig. 2). Crystals suitable for high-resolution diffraction data collection were obtained using the hanging-drop vapour-diffusion method by mixing 1 μl 60 mg ml⁻¹ protein solution and 1 μl reservoir solution consisting of 0.3 *M* ammonium acetate, 0.1 *M* bis-Tris pH 5.5, 26% (w/v) polyethylene glycol 3350. SDS-PAGE of the dissolved crystals was used to confirm that the complex had been crystallized (Fig. 3). Prior to data collection, the complex crystals were transferred to cryoprotectant solution consisting of 0.3 *M* ammonium acetate, 0.1 *M* bis-Tris pH 5.5, 30% (w/v) polyethylene glycol 3350, 5% dimethyl sulfoxide and soaked for about 1 min; they were then immediately flash-cooled in cryoloops in a liquid-nitrogen stream.

The data-collection statistics for the native crystal are given in Table 1. The crystal diffracted to 2.4 Å resolution (Fig. 4) and belonged to space group $P4_12_12$ or $P4_32_12$, with unit-cell parameters $a = 69.10$, $b = 69.10$, $c = 117.57$ Å. The asymmetric unit is estimated to contain one complex, with a corresponding Matthews coefficient of 2.13 Å³ Da⁻¹ and a solvent content of 47.56%.

The high quality of the data that we have collected has laid a solid foundation for the future structure determination of the complex between CCM3 and the C-terminal domain of MST4. Attempts to solve the structure of the complex using the 2.4 Å resolution data set are in progress.

The X-ray diffraction data sets were collected at the National Laboratory of Biomacromolecules, Institute of Biophysics, Chinese Academy of Sciences. The authors thank Yi Han of the Protein Platform of the Institute of Biophysics for providing the in-house X-ray facility for crystallographic analysis and data collection. This work was funded by the Chinese Ministry of Science and Technology

973 program (grants 2011CB910304 and 2011CB911103) and the Chinese Academy of Sciences (grant KSCX2-EW-J-3).

References

- Ceccarelli, D. F., Laister, R. C., Mulligan, V. K., Kean, M. J., Goudreault, M., Scott, I. C., Derry, W. B., Chakrabarty, A., Gingras, A. C. & Sicheri, F. (2011). *J. Biol. Chem.* **286**, 25056–25064.
- Fidalgo, M., Fraile, M., Pires, A., Force, T., Pombo, C. & Zalvide, J. (2010). *J. Cell Sci.* **123**, 1274–1284.
- Goudreault, M., D'Ambrosio, L. M., Kean, M. J., Mullin, M. J., Larsen, B. G., Sanchez, A., Chaudhry, S., Chen, G. I., Sicheri, F., Nesvizhskii, A. I., Aebersold, R., Raught, B. & Gingras, A. C. (2009). *Mol. Cell. Proteomics*, **8**, 157–171.
- He, Y., Zhang, H., Yu, L., Gunel, M., Boggon, T. J., Chen, H. & Min, W. (2010). *Sci. Signal.* **3**, ra26.
- Leslie, A. G. W. (2006). *Acta Cryst.* **D62**, 48–57.
- Louvi, A., Chen, L., Two, A. M., Zhang, H., Min, W. & Günel, M. (2011). *Proc. Natl Acad. Sci. USA*, **108**, 3737–3742.
- Revencu, N. & Vikkula, M. (2006). *J. Med. Genet.* **43**, 716–721.
- Voss, K., Stahl, S., Schleider, E., Ullrich, S., Nickel, J., Mueller, T. D. & Felbor, U. (2007). *Neurogenetics*, **8**, 249–256.
- Winn, M. D. *et al.* (2011). *Acta Cryst.* **D67**, 235–242.
- Zawistowski, J. S., Stalheim, L., Uhlik, M. T., Abell, A. N., Ancrile, B. B., Johnson, G. L. & Marchuk, D. A. (2005). *Hum. Mol. Genet.* **14**, 2521–2531.
- Zheng, X., Xu, C., Di Lorenzo, A., Kleaveland, B., Zou, Z., Seiler, C., Chen, M., Cheng, L., Xiao, J., He, J., Pack, M. A., Sessa, W. C. & Kahn, M. L. (2010). *J. Clin. Invest.* **120**, 2795–2804.